ISSN 1070-3284, Russian Journal of Coordination Chemistry, 2019, Vol. 45, No. 9, pp. 644–650. © Pleiades Publishing, Ltd., 2019.
Russian Text © The Author(s), 2019, published in Koordinatsionnaya Khimiya, 2019, Vol. 45, No. 9, pp. 546–552.

# Heterospin Cobalt, Nickel, and Copper Complexes: 4-TEMPO-Oxy-3,6-Di-*tert*-Butyl-*o*-Benzoquinone Derivatives

**N. O. Druzhkov[a], E. N. Nikolaevskaya[b], A. V. Cherkasova[a], K. A. Kozhanov[a, *], M. P. Bubnov[a], A. V. Cherkasov[a], A. S. Bogomyakov[c], and V. K. Cherkasov[a, **]**

[a] *Razuvaev Institute of Organometallic Chemistry, Russian Academy of Sciences, Nizhny Novgorod, 603600 Russia*

[b] *Zelinskii Institute of Organic Chemistry, Russian Academy of Sciences, Moscow, 119991 Russia*

[c] *International Tomography Center, Siberian Branch, Russian Academy of Sciences, Novosibirsk, Russia*

**e-mail: kostik@iomc.ras.ru*

***e-mail: cherkasov@iomc.ras.ru*

Received December 5, 2018; revised March 25, 2019; accepted April 4, 2019

**Abstract**—A series of heterospin bis-*o*-semiquinone cobalt, nickel, and copper complexes (4-TEMPO-oxy-3,6-di-*tert*-butyl-*o*-benzoquinone derivatives) is synthesized: (DMSO)Cu(4-TEMPO-O-3,6-DBSQ)$_2$ (**I**), (THF)$_2$Ni(4-TEMPO-O-3,6-DBSQ)$_2$ (**II**), (Py)$_2$Ni(4-TEMPO-O-3,6-DBSQ)$_2$ (**III**), and (Py)$_2$Ni(4-TEMPO-O-3,6-DBSQ)$_2$ (**IV**) (4-TEMPO-O-3,6-DBQ is 4-(3,6-di-*tert*-butyl-1,2-dioxocyclohexa-3,5-dien-4-yloxy)-2,2,6,6-tetramethylpiperidine-1-oxyl 4-oxy-2,2',6,6'-tetramethylpiperidine-1-oxyl). All complexes are characterized by elemental analysis, IR spectroscopy, magnetochemistry, and EPR. The structure of complex **I** is determined by X-ray diffraction analysis (CIF file CCDC no. 1882878). The coordination polyhedron of the copper atom in the molecular structure of the Cu(II) bis-*o*-semiquinone complex with dimethyl sulfoxide (DMSO) is a distorted tetragonal pyramid, whose equatorial plane contains the *o*-semiquinone ligands, and the DMSO molecule occupies the apical position. The magnetic properties of complexes **I**–**IV** are consistent with their compositions and structures. The magnetic behavior of copper complex **I** and nickel complexes **II** and **III** is determined by the balance of two contributions: metal–ligand ferromagnetic exchange interaction and ligand–ligand antiferromagnetic interaction. The temperature dependence of the magnetic moment of cobalt complex **IV** shows the redox isomeric transformation conjugated with the spin transition, which is characteristic of complexes of this type. No participation of nitroxyl radical centers is observed in intermolecular coordination.

*Keywords:* heterospin free radical complexes, *o*-semiquinones, nitroxyls, magnetic interactions, copper, cobalt, nickel

**DOI:** 10.1134/S1070328419090021

## INTRODUCTION

Biradical heterospin ligands containing two magnetic centers of different nature (each of which can bind with the metal) are of special interest as building blocks when constructing molecular magnetics [1–10]. We have recently synthesized new sterically hindered *o*-benzoquinone containing the 2,2,6,6-tetramethylpiperidineoxyl functional group and showed that its one-electron reduction is an efficient method for the generation of earlier unknown heterospin biradicals containing simultaneously nitroxyl and *o*-semiquinone radical centers [11]. Based on the known ability of nitroxyl radicals to act as ligands in coordination compounds [12–15], we synthesized a series of heterospin bis-*o*-semiquinone cobalt, nickel, and copper complexes, which are 4-TEMPO-oxy-3,6-di-*tert*-butyl-*o*-benzoquinone derivatives, in order to reveal the possible participation of the nitroxyl center in the formation of intermolecular coordination bonds.

## EXPERIMENTAL

All synthetic procedures were carried out in evacuated ampules in the absence of air oxygen and water traces. Solvents were purified using standard procedures [16]. Reagents and solvents were commercially available (Aldrich, Fluka, Stream). *o*-Quinone substituted by the TEMPO-O- fragment was prepared using a described procedure [11].

**Synthesis of (DMSO)Cu(4-TEMPO-O-3,6-DBSQ)$_2$ · 3DMSO (I).** Freshly purified metallic copper (wire) was placed in an evacuated ampule, and a solution of 4-TEMPO-O-3,6-DBQ (0.06 g, $1.54 \times 10^{-4}$ mol) in DMSO (10 mL) was added. The ampule was left to stay for 2 months at ambient temperature.

The reaction afforded the product as green laminated needles. The compound in the crystalline form is stable in air and highly soluble in organic solvents (except for saturated hydrocarbons), and its solutions are sensitive to air oxygen. The yield of compound **I** was 0.07 g (75%).

For $C_{54}H_{96}N_2O_{12}S_4Cu$

| | | | | |
|---|---|---|---|---|
| Anal. calcd., % | C, 56.05 | H, 8.36 | Cu, 5.49 | S, 11.08 |
| Found, % | C, 56.60 | H, 8.03 | Cu, 5.05 | S, 10.87 |

IR (ν, $cm^{-1}$): 1576 m, 1458 vs, 1359 s, 1331 s, 1288 m, 1238 m, 1186 s, 1091 s, 1060 m, 1022 s, 982 w, 951 m, 935 w, 914 w, 897 m, 843 m, 814 w, 794 w, 754 w, 721 w, 707 w, 692 w, 665 w, 634 w, 605 w, 588 w, 567 w, 516 w, 497 w.

**Synthesis of $(THF)_2$Ni(4-TEMPO-O-3,6-DBSQ)$_2$ (II).** Nickel carbonyl (0.077 g, 0.45 mmol) was condensed to a frozen solution of 4-TEMPO-O-3,6-DBQ (0.35 g, 0.9 mmol) in tetrahydrofuran (THF) (30 mL). When the reaction mixture was frozen out to room temperature, CO was evolved and the color of the solution changed to brown-green. After the end of gas evolution (~2 h), the reaction mixture was concentrated to 7–8 mL and the product was precipitated with hexane (50 mL). The yield of complex **II** as a green finely crystalline powder was 0.33 g (75%).

For $C_{54}H_{88}N_2O_{10}Ni$

| | | | | |
|---|---|---|---|---|
| Anal. calcd., % | C, 65.91 | H, 9.01 | N, 2.85 | Ni, 5.96 |
| Found, % | C, 66.07 | H, 9.13 | N, 2.63 | Ni, 5.68 |

IR (ν, $cm^{-1}$): 1576 m, 1489 s, 1458 vs, 1452 vs, 1363 m, 1356 m, 1327 s, 1242 m, 1230 m, 1196 m, 1184 s, 1090 s, 1051 w, 1026 w, 1006 w, 983 w, 916 m, 897 m, 839 w, 815 w, 794 w, 750 w, 721 w, 698 w, 680 w, 659 w, 603 w, 555 w, 515 w, 490 w.

**Synthesis of $(Py)_2$Ni(4-TEMPO-O-3,6-DBSQ)$_2$ (III).** Complex Ni(4-TEMPO-O-3,6-DBSQ)$_2$ · 2THF (SQ is the semiquinone ligand) (0.3 g, 0.3 mmol) was dissolved in pyridine (5 mL) placed in an evacuated ampule. The product was precipitated from the obtained solution by the slow addition of hexane (50 mL). The yield of complex **III** as a dark green finely crystalline powder was 0.27 g (89%).

For $C_{56}H_{82}N_4O_8Ni$

| | | | | |
|---|---|---|---|---|
| Anal. calcd., % | C, 67.40 | H, 8.28 | N, 5.61 | Ni, 5.88 |
| Found, % | C, 67.18 | H, 8.45 | N, 5.84 | Ni, 5.60 |

IR (ν, $cm^{-1}$): 1601 w, 1576 w, 1485 s, 1456 vs, 1363 m, 1323 m, 1228 m, 1217 m, 1182 m, 1082 m, 1139 w, 1024 w, 1006 w, 985 w, 966 w, 931 w, 912 w, 895 w, 760 w, 721 w, 700 m.

**Synthesis of (Bipy)Co(4-TEMPO-O-3,6-DBSQ)$_2$ (IV).** Dicobalt octacarbonyl (0.11 g, 0.32 mmol), 4-TEMPO-O-3,6-DBQ (0.5 g, 1.28 mmol), and 2,2'-bipyridyl (Bipy) (0.1 g, 0.64 mmol) were dissolved in THF (40 mL) in an evacuated ampule. The slow evolution of CO and a change in the solution color to gray-brown were observed within 4 h. After the end of gas evolution, the solvent was removed, the dry residue was dissolved in toluene (50 mL) on heating, and then a dark brown finely crystalline powder of complex **IV** (0.1 g, 0.64 mmol) was isolated from the obtained solution on cooling to −18°C in a yield of 0.48 g (75%).

For $C_{56}H_{80}N_4O_8Co$

| | | | | |
|---|---|---|---|---|
| Anal. calcd., % | C, 67.52 | H, 8.09 | N, 5.62 | Co, 5.92 |
| Found, % | C, 67.78 | H, 8.23 | N, 5.33 | Co, 5.71 |

IR (ν, $cm^{-1}$): 4500 br, 1601 w, 1570 m, 1558 m, 1448 vs, 1360 m, 1325 s, 1230 m, 1180 s, 1084 s, 1024 w, 1001 w, 980 m, 966 m, 893 w, 763 w, 731 w, 696 w, 652 w, 555 w.

IR spectra were recorded on an FSM 1201 instrument with FTIR transform in a range of 7000–400 $cm^{-1}$ (suspensions in Nujol). The magnetic susceptibility was measured on a Quantum Design MPMS XL SQUID magnetometer in a range of 2–300 K in a magnetic field of 5000 Oe. The diamagnetic corrections were applied using Pascal's constants. The effective magnetic moment was calculated by the equation $\mu_{eff}(T) = [(3k/N_A\mu_B^2)\chi T]^{1/2} \approx (8\chi T)^{1/2}$.

**The X-ray diffraction analysis** of the crystalline sample of complex **I** (0.4 × 0.4 × 0.1 mm) was carried out on a Bruker D8 Quest diffractometer (ω scan mode, Mo$K_\alpha$ radiation, λ = 0.71073 Å, $T$ = 100 K, 2θ = 50.13°). The experimental sets of intensities were measured and integrated, an absorption correction was applied, and the structure was refined using the APEX3 [17], TWINABS [18], SHELX [19] program packages. The crystals of complex **I** were monoclinic ($C_{48}H_{78}CuN_2O_9S$, $3C_2H_6OS$), space group $P2_1/c$, $a$ = 18.8866(13), $b$ = 29.781(2), $c$ = 11.3819(8) Å, β = 104.529(2)°, $V$ = 6197.2(8) $Å^3$, $Z$ = 4, $\rho_{calcd}$ = 1.240 $mg/m^3$, μ = 0.543 $mm^{-1}$. The structure was refined as a merohedral twin (HKLF 5) with the domain ratio 0.72 : 0.28, and 13073 independent reflections ($R_{int}$ = 0.0789) were used for the refinement of 763 parameters of the structure by full-matrix least squares for $F_{hkl}^2$ in the anisotropic approximation for non-hydrogen atoms. Hydrogen atoms were placed in the geometrically calculated positions and refined isotropically with fixed thermal parameters $U(H)_{iso}$ = $1.2U(C)_{eq}$ ($U(H)_{iso} = 1.5U(C)_{eq}$ for methyl groups). An analysis of the electron density synthesis showed that one of the *tert*-butyl substituents and all DMSO molecules including that coordinated on the copper(II) atom were disordered. Two positions were localized for each disordered fragments. The DFIX, EADP, ISOR, and RIGU instructions were used to restraint

geometric and anisotropic parameters of atomic shifts in the disordered fragments. After the final refinement, $S(F^2) = 1.085$ and $R_1 = 13.3\%$ (for all reflections satisfying the condition $I > 2\sigma(I)$). Unfortunately, lower values of convergence factors were not attained because of the insufficient quality of the crystalline samples (the completeness of data collection was 90%) and many disordered fragments. The residual electron density maximum and minimum were 1.76 and –0.92 e/Å$^3$, respectively.

The structure of complex **I** was deposited with the Cambridge Crystallographic Data Centre (CIF file CCDC no. 1882878; ccdc.cam.ac.uk/getstructures).

## RESULTS AND DISCUSSION

Copper complex **I** was prepared by the dissolution of metallic copper in a solution of *o*-quinone in DMSO. Complex **II** was synthesized by the reaction of nickel tetracarbonyl with *o*-quinone containing the free radical nitroxyl substituent in THF. The reaction of complex **II** with pyridine affords complex **III**. The cobalt bis-*o*-quinone complex with 2,2'-bipyridyl (**IV**) was synthesized by the reaction of the corresponding *o*-quinone with dicobalt octacarbonyl in the presence of 2,2'-bipyridyl (Schemes 1–3).

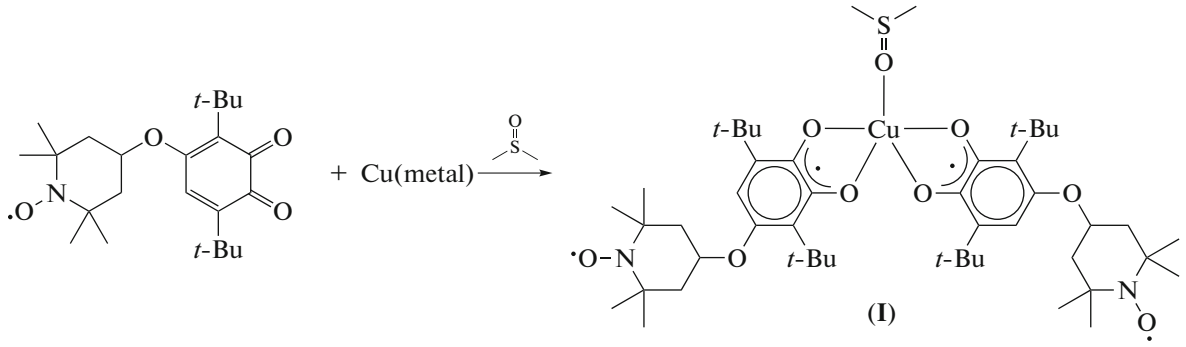


**Scheme 1.**

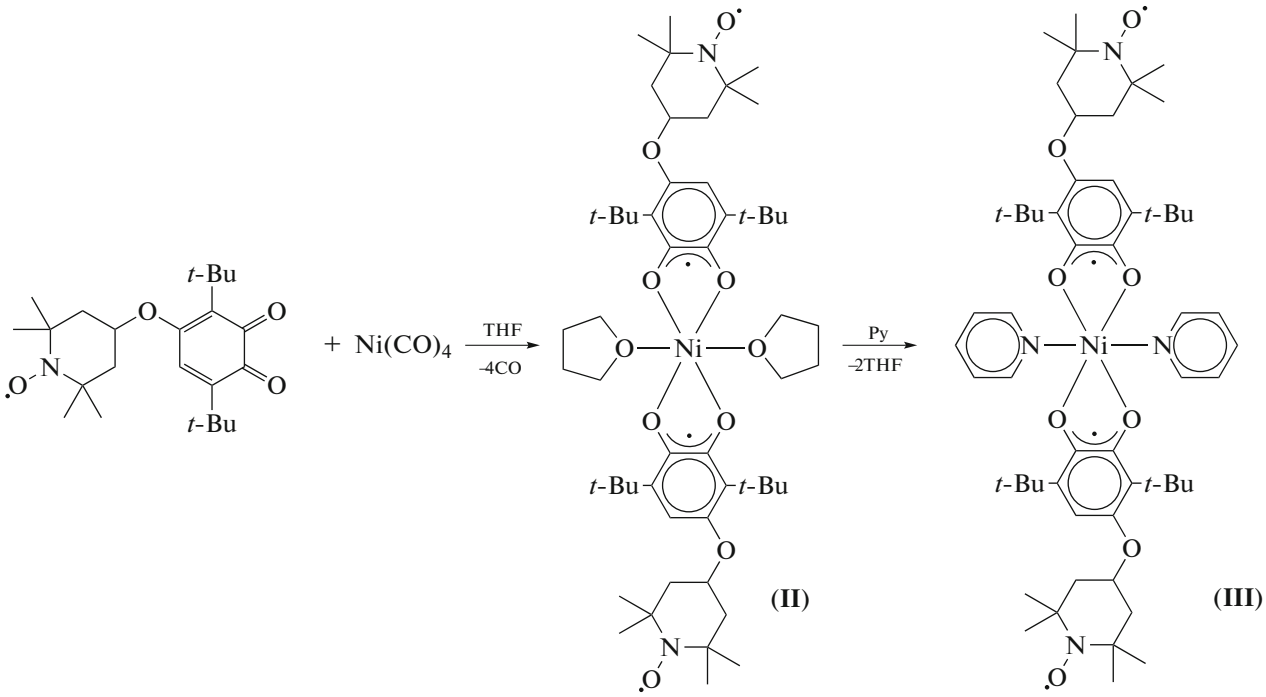


**Scheme 2.**

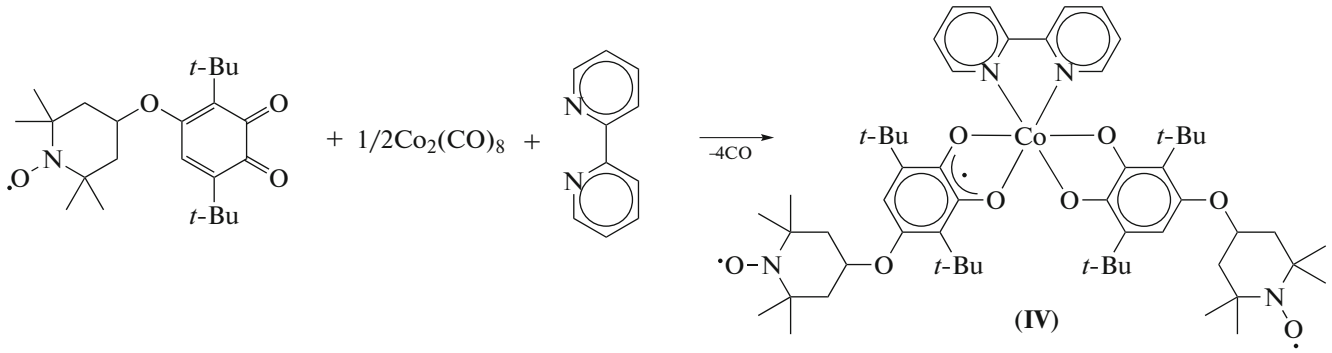


**Scheme 3.**

The redox isomerism equilibrium for complex **IV** can be presented by Scheme 4

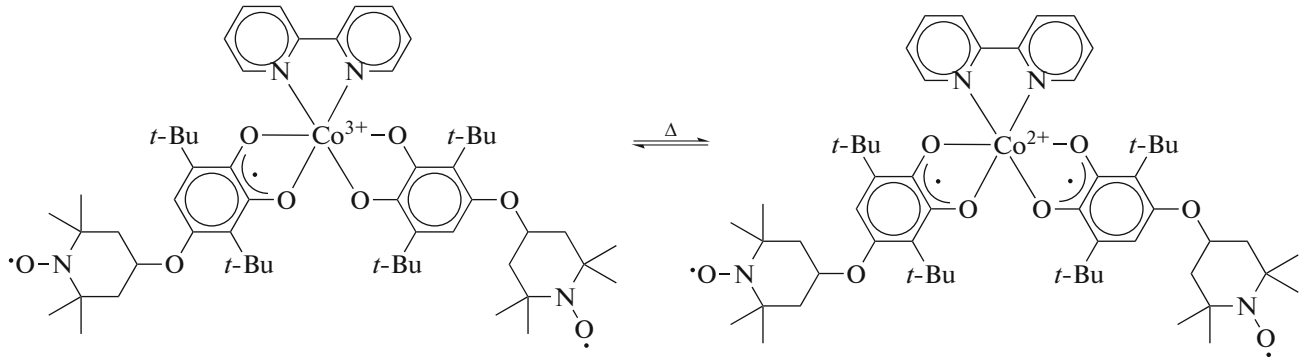


**Scheme 4.**

All complexes were isolated in the individual state and characterized by elemental analysis, IR spectroscopy, and magnetometry. The single-crystal X-ray diffraction analysis was carried out for copper complex **I**. The IR spectra of complexes **I**–**IV** correspond to their compositions. All spectra are characterized by the predominant intensity band at 1450 $cm^{-1}$ assigned to stretching vibrations of the sesquialteral C–O bond typical of SQ ligands [20]. The nitroxyl group of the TEMPO fragment is observed in the IR spectra as a band corresponding to stretching N–O vibrations at 1364 $cm^{-1}$ [21]. In complex **I**, DMSO is observed by a broad band in a range of 3490–3290 $cm^{-1}$, as well as at 1020 and 950 $cm^{-1}$. In complex **II**, THF is determined by the intense band at 1090 $cm^{-1}$. Pyridine in complex **III** can be characterized by bands at 1600, 1082, and 702 $cm^{-1}$. The spectrum of complex **IV** exhibits a broad ligand-to-ligand charge-transfer band at 4500 $cm^{-1}$ characteristic of the cobalt catecholate-*o*-semiquinone complexes [22] and bands at 1601, 763, and 732 $cm^{-1}$ assigned to the bipyridyl ligand.

Unfortunately, we failed to obtain crystals of complexes **II**–**IV** suitable for X-ray diffraction analysis. According to the X-ray diffraction data, compound **I** is a complex in which the $Cu^{2+}$ cation is bound to two semiquinone ligands and one DMSO molecule. The independent part of the crystal cell contains one complex molecule and three solvate molecules of DMSO. The coordination polyhedron of divalent copper in complex **I** (Fig. 1) is a distorted tetragonal pyramid, the base of which is formed by the oxygen atoms of the SQ ligands, and the oxygen atom of the DMSO molecule lies at the axial vertex. Each DMSO molecule, including that coordinated on the copper atom, is disordered over two positions. The Cu–O(SQ) bond lengths lie in a narrow range of 1.926(7)–1.951(7) Å, and the Cu–O(DMSO) distance is 2.237(7) Å. The electron density delocalization over the OCCO fragment is observed in the semiquinone ligands: the C–O and C–C bond lengths are 1.28(2)–1.31(2) and 1.46(2)–1.47(2) Å, respectively, indicating the radical anion form of coordination [23, 24]. The dihedral angle between the OCCO planes of the semiquinone ligands is 29.5(6)°, and the O(SQ)CuO(DMSO) angles lie in a range of 93.1(3)°–100.4(3)°.

The TEMPO fragment in the semiquinone ligands exists in the chair conformation. The dihedral angles between the mean planes passing through the carbon ring of the semiquinone fragment and the heterocycle of the TEMPO fragment are 61.3(4)° and 47.6(4)°. The O(3)–C(SQ) and O(7)–C(SQ) bonds are significantly shorter (1.35(2)–1.37(2) Å) than O(3)–C(TEMPO) and O(7)–C(TEMPO) (1.45(2)–1.47(2) Å).

The crystal packing of complex **I** contains multiple contacts O···H and H···H predominantly between the complex molecule and DMSO molecules. The O···H

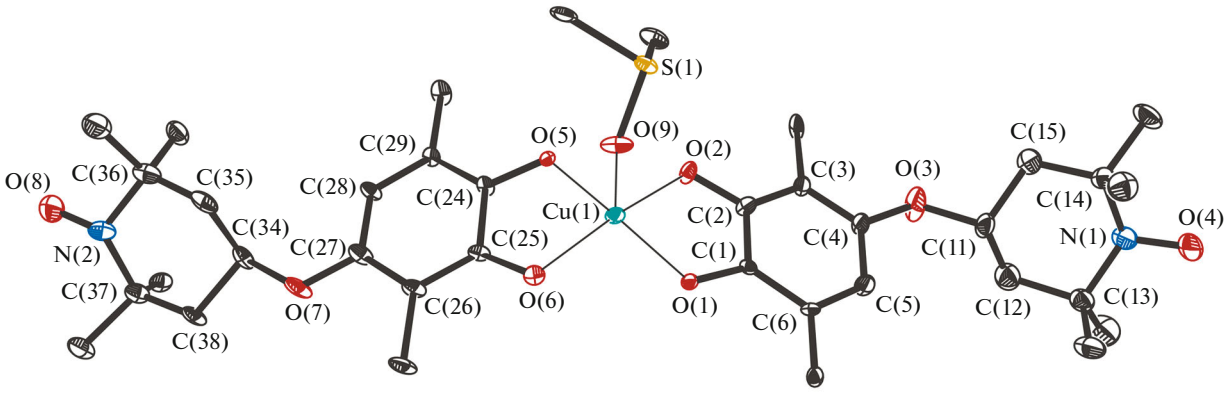


**Fig. 1.** Molecular structure of complex **I**. Thermal ellipsoids of 30% probability. Hydrogen atoms and methyl groups of the *tert*-butyl substituents are omitted for clarity.

and H···H distances lie in the ranges 2.46(2)–2.64(2) and 2.18(2)–2.40(2) Å, respectively.

The temperature dependences of the magnetic moments for complexes **I**–**IV** (Fig. 2) are similar to that for the earlier described bis-*o*-semiquinone complex Cu(3,6-DBSQ)$_2$(3,6-DBSQ is 3,6-di-*tert*-butyl-*o*-benzoquinone) [25], whose magnetic properties are determined by the balance of the ferromagnetic (metal–ligand) and antiferromagnetic (ligand–ligand) channels of exchange interactions. The magnetic moment of complex **I** at 300 K is 4.03 $\mu_B$ and decreases as the temperature decreases reaching a plateau of ~2.87 $\mu_B$ at temperatures below 30 K. The high-temperature value is close to the theoretical one (3.93 $\mu_B$) for five noninteracting paramagnetic centers with the spins $S = 1/2$: two nitroxyls ($g_R = 2$), two semiquinone ligands ($g_{SQ} = 2$), and one $Cu^{2+}$ ($g_{Cu} = 2.15$). The decrease with a decrease in temperature indicates strong exchange interactions of the antiferromagnetic character. The trimer model ($H = -2J_{Cu\text{-}SQ}(S_{SQ1}S_{Cu} + S_{Cu}S_{SQ2}) - J_{SQ\text{-}SQ}S_{SQ1}S_{SQ2}$) taking into account the paramagnetic contribution from the spins of nitroxyls according to the Curie law was used to analyze the $\mu_{eff}(T)$ dependence. The optimum values of the $g_{Cu}$, $J_{Cu\text{-}SQ}$, and $J_{SQ\text{-}SQ}$ and $C$ parameters are 2.31, 336, and −212 cm$^{-1}$ and 0.542 K cm$^3$/mol, respectively, and are comparable with the corresponding values for the earlier described complex Cu(3,6-DBSQ)$_2$ [25]. The value of the Curie constant $C$ is slightly lower than the theoretical spin-only value (0.75 K cm$^3$/mol) for two noninteracting nitroxyls.

The magnetic behavior of complexes **II** and **III** is characteristic of other known nickel complexes with THF and pyridine. The general views of the $\mu_{eff}$–$T$ curves for complexes **II** and **III** (Fig. 2) resemble those for previously described *cis*-(THF)$_2$Ni(3,6-DBSQ)$_2$ [26] and *trans*-(Py)$_2$Ni(3,6-DBSQ)$_2$ [27], respectively. The values of $\mu_{eff}$ for complexes **II** and **III** at room temperature are 4.78 and 5.13 $\mu_B$, respectively. Both values exceed the spin-only value equal to 4.47 $\mu_B$, which was calculated for the system of noninteracting spins: high-spin $d^8$ $S = 1$; 2 SQ $S = 1/2$; and 2 TEMPO $S = 1/2$, indicating that the ferromagnetic exchange interactions predominate. The magnetic moment increases as the temperature decreases and reaches a maximum of 5.37 $\mu_B$ at 5 K for complex **II** and 5.25 $\mu_B$ in a range of 100–180 K for complex **III**. The further decrease in temperature results in a sharp decrease in the magnetic moment for complex **II** and a smooth decrease for complex **III** to 5.25 and 3.16 $\mu_B$ (2 K), respectively. This difference in behavior shows

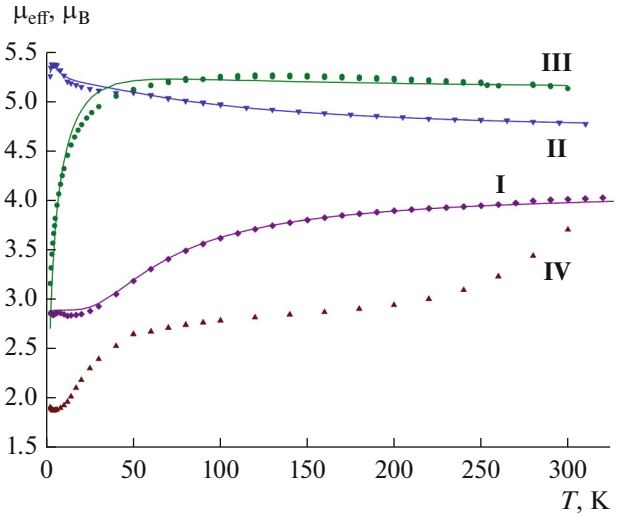


**Fig. 2.** Temperature dependences of the magnetic moments for complexes **I**–**IV** (approximated curves are shown by dotted lines).

different ratios of the energies of the ferro- and antiferromagnetic interactions in molecules of the complexes. The approximation gives the following values:

$(THF)_2Ni(SQ)_2$: $J_{Ni\text{-}SQ}$ = 18.8 $cm^{-1}$; $J_{SQ\text{-}SQ}$ = $-16.9\ cm^{-1}$; $g_{Ni}$ = 2.2 (fix.); $g_{SQ}$ = 2.00 (fix.); $zJ'$ = $-0.01\ cm^{-1}$.

$(Py)_2Ni(SQ)_2$: $J_{Ni\text{-}SQ} = 261\ cm^{-1}$; $J_{SQ\text{-}SQ} = -233\ cm^{-1}$; $g_{Ni} = 2.2$ (fix.); $g_{SQ} = 2.00$ (fix.); $zJ' = -0.44\ cm^{-1}$.

Complex **IV** exhibits a more complicated magnetic behavior. Complex **IV** is analogous in composition to the redox isomeric compound (Bipy)Co(3,6-DBSQ)$_2$ [28–30] for which the critical temperature is $T_{cr}$ = 300 K.

$$\underset{\text{Co(III), } d^6\text{, low-spin}}{\text{(Bipy)Co(3,6-DBCat)(3,6-DBSQ)}} \overset{\Delta}{\rightleftharpoons} \underset{\text{Co(II), } d^7\text{, high-spin}}{\text{(Bipy)Co(3,6-DBSQ)}_2}$$

In a range of 50–200 K, the magnetic moment of complex **IV** changes slightly and is equal to 2.64–2.94 $\mu_B$. This value is close to the theoretical one calculated for three noninteracting lone electrons (3.0 $\mu_B$), which corresponds to the system of spins: low-spin Co(III) $d^6$ $S$ = 0; 1 SQ $S$ = 1/2; and 2 TEMPO $S$ = 1/2, i.e., to the low-temperature redox isomer. Heating leads to an increase in the magnetic moment to 3.7 $\mu_B$ at 300 K. On cooling below 50 K, the magnetic moment decreases to 1.87 $\mu_B$ at 5 K. Thus, on cooling the antiferromagnetic exchange results in the situation where the single lone electron remains, most probably, on the *o*-semiquinone fragment, whose participation in intermolecular interactions is highly improbable. Heating above 200 K leads to the shift of the redox isomerism equilibrium to the high-spin Co(II) isomer: high-spin Co(II) $d^7$ $S$ = 3/2; 2 SQ $S$ = 1/2; and 2 TEMPO $S$ = 1/2. Evidently, at 300 K the redox isomeric transformation is far from completion.

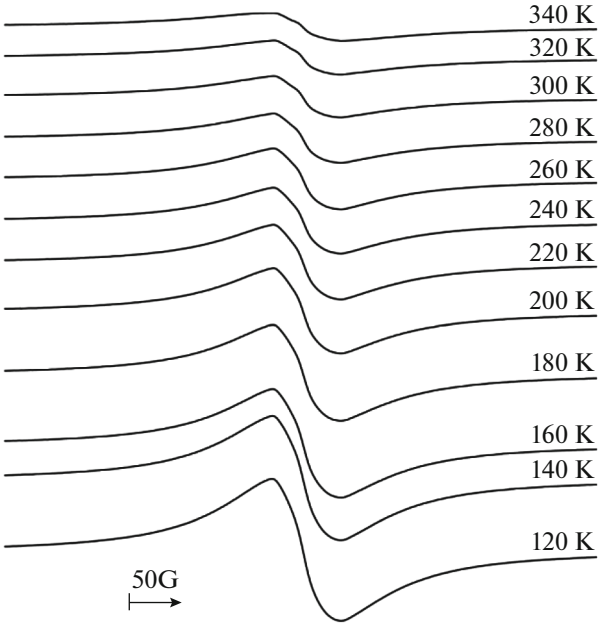


**Fig. 3.** General view of the EPR spectra of complex **IV** in the range 120–340 K.

The EPR spectrum of powdered complex **I** represents a single line without a structure ($g_i$ = 2.0064, linewidth ~14 Oe), whose width and intensity do not substantially change with temperature. Powdered complexes **II** and **III** have no EPR spectra, which is not surprising for the high-spin nickel complexes.

The spectrum of the powdered sample of complex **IV** in a range of 120–340 K is a broad (linewidth ~50 Oe) signal with $g_i \approx 2.0045$ and a weakly resolved hyperfine structure (Fig. 3). The signal intensity decreases with temperature without a change in the linewidth.

However, the $IT$ dependence ($I$ is the double integral intensity) on temperature ($T$) (Fig. 4) indicates that the amount of paramagnetic particles in the sample giving the EPR signal remains approximately unchanged in a range of 120–200 K. The observed sharp decrease in the intensity at the temperatures above 220 K can be explained by the redox isomeric transformation leading to the formation of high-spin particles having no EPR signal.

The EPR spectra of the complexes in solutions are presented by the spectrum of the nitroxyl ligand.

Thus, the reduction of 4-TEMPO-oxy-3,6-di-*tert*-butyl-*o*-benzoquinone by metallic copper, $Ni(CO)_4$, and $Co_2(CO)_8$ affords the corresponding multispin metal complexes containing the biradical heterospin

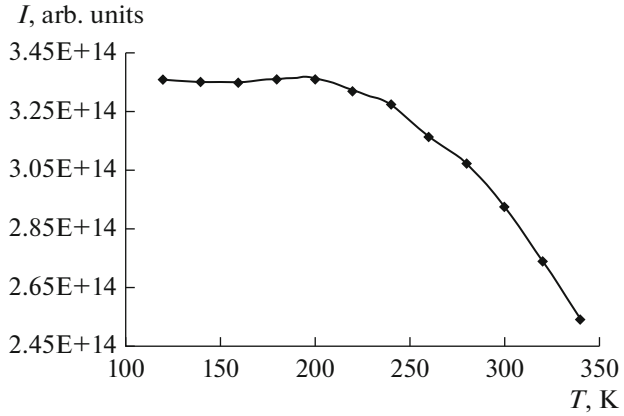


**Fig. 4.** Temperature dependence of the double integral intensity of the EPR spectrum of powdered complex **IV**.

ligands. An analysis of the molecular structure and magnetic properties of new complexes indicates a magnetic structural relationship inherent in the analogs of the complexes without the nitroxyl substituent in the *o*-semiquinone ligand. No participation of nitroxyl radical centers in intermolecular coordination was observed.

## ACKNOWLEDGMENTS

The X-ray diffraction studies were carried out using the scientific equipment of the Center for Collective Use "Analytical Center of the Razuvaev Institute of Organometallic Chemistry of the Russian Academy of Sciences."

## FUNDING

This work was supported by the Russian Science Foundation, project no. 14-13-01296. The X-ray diffraction studies were carried out in terms of the state task (theme no. 44.2, registration no. AAAA-A16-116122110053-1).

## CONFLICT OF INTEREST

The authors declare that they have no conflicts of interest.

## REFERENCES

1. Eaton, S.S., *Coord. Chem. Rev.*, 1978, vol. 26, p. 20.
2. Eaton, S.S. and Eaton, G.R., *Coord. Chem. Rev.*, 1988, vol. 83, p. 29.
3. Artemrev, A.V., Vysotskaya, O.V., Oparina, L.A., et al., *Polyhedron*, 2016, vol. 119, p. 293.
4. Shultz, D.A., Bodnar, S.H., Vostrikova, K.E., et al., *Inorg. Chem.*, 2000, vol. 39, p. 6091.
5. Depperman, E., Bodnar, S.H., Vostrikova, K.E., et al., *J. Am. Chem. Soc.*, 2001, vol. 123, p. 3133.
6. Shultz, D., Vostrikova, K., Bodnar, S., et al., *J. Am. Chem. Soc.*, 2003, vol. 125, p. 1607.
7. Kirk, M.L., Shultz, D.A., and Depperman, E.C., *Polyhedron*, 2005, vol. 24, p. 2880.
8. Shultz, D.A., Kumar, R.K., Bin-Salamon, S., and Kirk, M.L., *Polyhedron*, 2005, vol. 24, p. 2876.
9. Stasiw, D.E., Zhang, J., Wang, G., Dangi, R., et al., *J. Am. Chem. Soc.*, 2015, vol. 137, p. 9222.
10. Tret'yakov, E.V., Tolstikov S.E., Romanenko G.V., et al., *Izv. Akad. Nauk, Ser. Khim.*, 2011, p. 2280.
11. Egorova, E.N., Druzhkov, N.O., Kozhanov, K.A., et al., *Izv. Akad. Nauk, Ser. Khim.*, 2017, p. 1629.
12. Dickman, M.H. and Doedens, R.J., *Inorg. Chem.*, 1982, vol. 21, p. 682.
13. Jaitner, P., Huber, W., Huitner, G., and Scheidsteger, O., *J. Organomet. Chem.*, 1983, vol. 259, p. C1.
14. Jaitner, P., Huber, W., Gieren, A., et al., *J. Organomet. Chem.*, 1986, vol. 311, p. 379.
15. Isrow, D. and Captain, B., *Inorg. Chem.*, 2011, vol. 50, p. 5864.
16. Armarego, W.L.F. and Chai, C.L.L., *Purification of Laboratory Chemicals*, Oxford: Elsevier, 2009.
17. *APEX 3. Version 2016-9*, Madison: Bruker AXS Inc., 2016.
18. *TWINABS. Version 2012/1*, Madison: Bruker AXS Inc., 2012.
19. Sheldrick, G.M., *Acta Crystallogr., Sect. C: Struct. Chem.*, 2015, vol. 71, p. 3.
20. Bubnov, M.P., Skorodumova, N.A., Arapova, A.V., et al., *Z. Anorg. Allg. Chem.*, 2014, p. 2177.
21. Kasumov, V.T., Uçar, I., Bulut, A., and Yerli, Y., *Solid State Sci.*, 2011, vol. 13, p. 1852.
22. Pierpont, C.G. and Kelly, J.K., *Coordination Chemistry of o-Semiquinones. PATAI'S Chemistry of Functional Groups*, Wiley, 2013, p. 13.
23. Pierpont, C.G. and Buchanan, R.M., *Coord. Chem. Rev.*, 1981, vol. 38, p. 45.
24. Brown, S.N., *Inorg. Chem.*, 2012, vol. 51, p. 1251.
25. Ovcharenko, V.I., Gorelik, E.V., Fokin, S.V., et al., *J. Am. Chem. Soc.*, 2007, vol. 129, p. 10512.
26. Piskunov, A.V., Fukin, G.K., Kurskiiyu, A., et al., *Inorg. Chem. Commun.*, 2005, vol. 8, p. 339.
27. Bubnov, M., Cherkasova, A., Teplova, I., et al., *Polyhedron*, 2016, vol. 119, p. 317.
28. Abakumov, G.A., Cherkasov, V.K., Bubnov, M.P., et al., *Dokl. Akad. Nauk SSSR*, 1993, vol. 330, p. 332.
29. Lebedev, B.V., Smirnova, N.N., Abakumov, G.A., et al., *J. Chem. Thermodyn.*, 2002, vol. 34, p. 2093.
30. Bubnov, M.P., Skorodumova, N.A., Arapova, A.V., et al., *Inorg. Chem.*, 2015, vol. 54, p. 7767.

*Translated by E. Yablonskaya*